Asian Journal of Chemistry; Vol. 23, No. 3 (2011), 1247-1251

ASIAN JOURNAL OF CHEMISTRY

www.asianjournalofchemistry.co.in

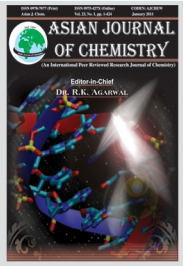

$LaMn_{1-x}Cu_xO_3$ Perovskite Catalysts Prepared for Volatile Organic Compounds Combustion

YULIN GU[1,2], YUXIA YANG[1], YANMING QIU[1], KUNPENG SUN[1] and XIANLUN XU[1,*]

[1]State Key Laboratory for Oxo Synthesis and Selective Oxidation, Lanzhou Institute of Chemical Physics, Chinese Academy of Science, Lanzhou 730000, P.R. China
[2]Graduate School of the Chinese Academy of Sciences, Beijing 100039, P.R. China

*Corresponding author: Fax: +86 931 4968010; Tel: +86 931 4968217; E-mail: guyulin@gmail.com

(*Received*: 29 April 2010; *Accepted*: 6 November 2010) AJC-9279

A series of Al_2O_3 immobilized La-Mn-Cu-O catalysts were prepared by impregnation method and their performance in ethyl acetate catalytic combustion was investigated. The ethyl acetate been completely converted exclusively into H_2O and CO_2 on $LaMn_{0.6}Cu_{0.4}O_3/Al_2O_3$ catalyst with long life. Highly dispersed perovskite phase was detected by detailed analysis using the methods of X-ray diffraction, X-ray photoelectron spectroscopy and scanning electron microscopy. The different activities of the various catalysts were due to the changed contents and mobility of active oxygen of the catalysts, which induced by the partial substitution of Mn by Cu ion.

Key Words: Catalytic combustion, Ethyl acetate, Perovskite, Catalyst.

INTRODUCTION

Volatile organic compounds (VOCs) are toxic pollutant to environment and produced in variety of small and medium size industries. Used as the common solvent, ethyl acetate was presented in various gas exhaust stream, often cause severe environmental hazards and be harmful to the health of human being. Among the several techniques that can efficiently control the emission of VOCs, catalytic combustion is one of the competitive arts to meet the stricter environmental legislations. Traditionally the catalysts employed for VOCs removal are mainly noble metal catalysts due to their high activity. Recently, it was reported that supported no noble metal oxide could also be good catalyst in VOCs combustion[1-3]. Among them, perovskite-type materials had proved to be an interesting catalyst for completely catalytic oxidation[4-8], being cheaper, comparatively active and much more resistant to deactivation than the traditional noble metal catalyst.

Perovskite is mixed metal oxide with general formula of ABO_3, where B is usually a transition metal cation, surrounded by six oxygen in octahedral coordinated ions and A is a rare-earth metal cation, 12-coordinated by oxygen, which occupies the cavities made by the BO_6 octahedral. It had been extensively studied for their physical and technological properties. Both A and B metal ions can be partially substituted, leading to a wide variety of structures. These often characterized by oxygen non-stoichiometry, which determines the interesting catalytic properties for many reactions[9]. Many efforts were made in order to improve the activity by partial substitution of A cation by cation of different valence, like Sr^{2+} and Ce^{4+} [10-14].

Among the perovskite materials, those containing lanthanum and manganese have received much more attention in both fundamental and applied science, since they are less expensive and often more thermally stable than noble metals. More importantly, some results possess similar or higher activity than Pt-supported catalyst[15-16]. As the active phase, $LaMnO_3$ in the catalytic combustion of alkane and alkene had been extensively investigated in recent years[17-20], substitution of Mn by transition metal ion on perovskite-type compounds had been investigated intensively for their wide range shift of oxidative (excess of oxygen) and reductive (oxygen deficiency) non-stoichiometry which can enhance the catalytic performance of the materials. Modification in other properties of $LaMnO_3$ perovskite oxide, such as oxygen content and catalytic activity, considered to been affected by the crystal structure changes induced by variation in Mn valence and the crystal structure of the perovskite[21,22].

In this paper, the catalytic performance of various $LaMn_{1-x}Cu_xO_3$ perovskite catalysts is investigated for ethyl acetate combustion reaction and also characterized the catalysts using the methods of XRD, XPS and SEM to monitor the effect of substitution of Mn site by Cu on the catalytic properties.

EXPERIMENTAL

Samples of Al_2O_3 (commercial alumina) supported $LaMn_{1-x}Cu_xO_3$ with nominal composition x = 0, 0.2, 0.3, 0.4

and 0.5 have been prepared by impregnation method. In the first case, impregnated Al_2O_3 with desired concentrations of $La(NO_3)_3$, $Mn(NO_3)_2$ and $Cu(NO_3)_2$ aqueous solutions for 24 h and dried at 120 ºC for 6 h, followed the calcinations in a muffle furnace with an air stream at 700 ºC for 4 h. Finally, the samples cooled to room temperature. The supported catalysts with different perovskite loadings were denoted as Cat. 0, Cat. 2, Cat. 3, Cat. 4 and Cat. 5 with the value of x = 0, 0.2, 0.3, 0.4 and 0.5, respectively. For comparison purpose, bulk perovskite prepared by the citrate methods. $La(NO_3)_3$, $Mn(NO_3)_2$, $Cu(NO_3)_2$ and citric acid were dissolved in de-ionized water in stoichiometric proportion; citric acid/metal ion mole ratio is 1.5. The solution evaporated at 80 ºC and the final gel calcined at 700 ºC for 4 h. Then, it was ground and sieved for further use.

General procedure: The combustion reaction performed in a quartz tubular fixed-bed reactor (400 mm length, 6 mm internal diameter) at atmospheric pressure. The reaction gas was self-made with contents of 0.2 % ethyl acetate and 99.8 % air. The space velocity is 12000 mL/h/mL and 0.5 g catalyst used. A thermocouple placed inside the reactor, in the center of the catalyst bed to monitor the reaction temperature. Reaction temperature ranged from 100-400 ºC. All experiment runs under a steady-state condition. The products analyzed on-line by gas chromatograph, equipped with a TDX column connected to a TCD for CO_2 determination and a FFAP column used to separate the different components in reaction mixture.

Detection method: X-Ray diffraction (XRD) patterns obtained with a Shimadzu XD-3A diffraction meter employing Ni-filtered CuK_α radiation (0.15418 nm). The X-ray tube operated at 35 KV and 15 mA. Raman spectra measured on a Perkin-Elmer 2000 Raman spectrometer with diode-pumped YAG laser and a RT super Incas detector. The laser power was 50-400 mW. BET specific surface areas determined by nitrogen adsorption at the temperature of liquid nitrogen on a Micromeritics ASAP 2000 instrument. Prior to each analysis the catalyst powder was degassed at 150 ºC under a pressure of 0.1 Pa for 2 h. X-Ray photoelectron spectroscopic (XPS) results obtained using a V.G. Escalab MK II spectrometer equipped with a hemispherical electron analyzer. The system was operated at 13 kV and 20 mA using a magnesium anode (Mg k, E = 1253.6 eV). A binding energy (BE) of 285 eV for the C1s level used as an internal reference. The morphology of the samples was analysed by SEM, on a Jeol model JSM-5400 LV microscope.

RESULTS AND DISCUSSION

The catalytic activity of ethyl acetate combustion was measured on the supported catalysts $LaMn_{1-x}Cu_xO_3/Al_2O_3$ with different X values (X = 0, 0.2, 0.3, 0.4, 0.5). The main products detected in all experimental conditions were only CO_2 and H_2O when the total conversion reached to 100 %, except small amounts of by-products, such as ethanol and acetaldehyde, detected at lower temperature. Table-1 indicated that the by-products were far below the detected level for the 10 % perovskite catalyst at T_{100} (the temperature at which the conversion level is 100 %). Fig. 1 shows the dependence of ethyl acetate conversion on the reaction temperature for the prepared

TABLE-1
ACTIVITY DATA OF THE CATALYSTS WITH DIFFERENT LOADING PER CENT

Percent (%)	T_{50} (%)*				T_{100} (%)*			
	CO_2	CH_3CHO	C_2H_5O	H_2	CO_2	CH_3CHO	C_2H_5O	H_2
5	21	12	8	9	89	6	2	3
10	45	4	1	–	100	–	–	–
20	37	10	3	–	97	2	1	–
100	21	14	11	4	95	3	1	1

*T_{50} and T_{100} data Fig. 1.

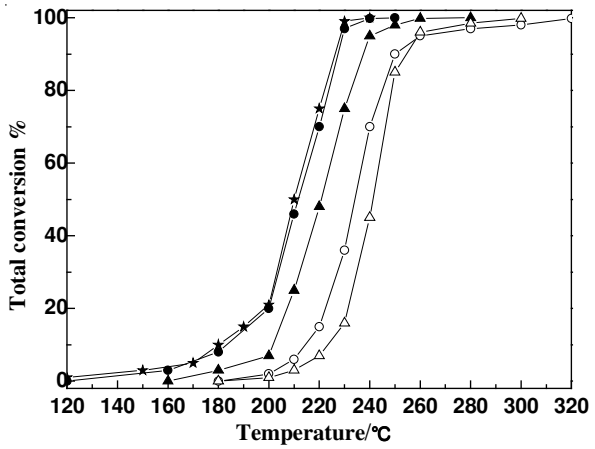

Fig. 1. Catalytic activity for combustion of ethyl acetate on $LaMn_{1-x}Cu_xO_3/Al_2O_3$ catalysts with different x value: (★)x = 0.5; (●) x = 0.4; (▲) x = 0.3; (○) x = 0.2; (△) x = 0

catalysts with different X value. The presence of Cu improved the catalytic activity. The catalytic performance vary in the investigated range of copper content, results showed that higher activity was obtained for the samples with the x value of 0.4 and 0.5. This result can be tentatively justified with some different structure of the solid containing, such as a crystalline phase and the various surface properties, which could show by XRD and XPS analysis. For the sake of clarity, light-off temperatures T_{50} reported in Fig. 2 as a function of the copper content. Obviously, the catalytic activity of the catalyst increased with the Cu content. We proposed that the role of the Cu^{2+} substitution correlated with the formation of Mn^{4+} cation and the fixation of the oxygen stoichiometry of the catalysts. Cu improves the catalytic activity due to the partial substitution of Mn ion.

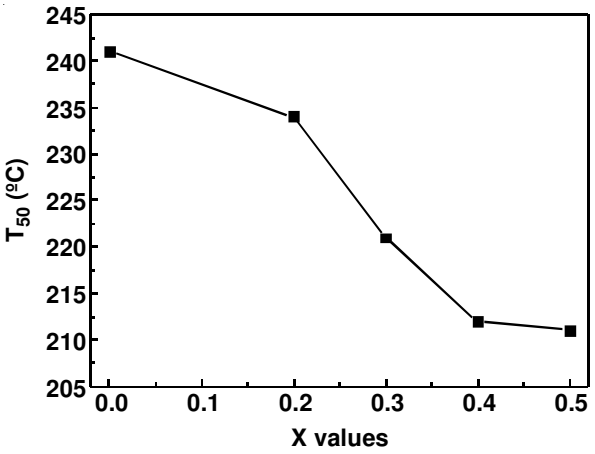

Fig. 2. Light-off temperature T_{50} as a function of X value

Table-2 lists the XRD phases and the surface area of the catalysts. The result show that a calcinations temperature of 700 ºC is insufficient to obtain an evident perovskite phase for Cat. 2, but both Cat. 3 and Cat. 4 samples displayed the obvious perovskite phase signals. The γ-Al_2O_3 used as support has a poorly crystalline structure with the BET area of 156 m^2/g. The specific surface area of Cat. 4 decreased obviously when the calcination temperature is higher than 800 ºC. The decrease in specific surface area observed at higher calcination temperature is the result of two different processes: a crystal domain size enlarged and an increase of the fraction of surface lost by adhesion of nano-sized domains inside the agglomerates. We know that certain relation existed between the activity and the BET area. For Cat. 4, the deposition of perovskite phase on alumina does not promoted any phase transition of the support upon calcinations at 800 ºC, but a dramatic reduction of the surface area was observed. Furthermore, no signals of the perovskite phase detected, due to dilution effect or the fact that X-ray diffractogram recorded on powders obtained by crushing the balls. The dispersion degree of perovskite phase cannot ignore. Moreover, in this case the presence of the active phase may enhance the reaction between lanthanum and aluminum oxides, leading to the formation of $LaAlO_3$ and other aluminum-lanthanum mixed oxides. Nevertheless, we cannot totally exclude the possible formation of small particles of these compounds on the samples only by the XRD data. Although no signals of lanthanum and manganese-oxide detected from all catalysts. We examined the valence states

TABLE-2
SURFACE AREA AND XRD PHASES OF $LaMn_{1-x}Cu_xO_3/Al_2O_3$ CATALYSTS

Catalyst	X Value	XRD Phase	Total pore volume ($mL\ g^{-1}$)	Calcinations temp. (ºC)	BET ($m^2\ g^{-1}$)
Cat. 0	0	γ	0.3012	700	98.12
Cat. 2	0.2	γ	0.3100	700	99.61
Cat. 3	0.3	P, γ	0.3154	700	100.11
Cat. 4	0.4	P, γ	0.3195	700	100.73
Cat. 4	0.4	P, γ	0.3099	800	80.14
Al_2O_3	–	γ	0.4493	700	156.03

P: $LaMnO_3$ perovskite; γ: Alumina phase.

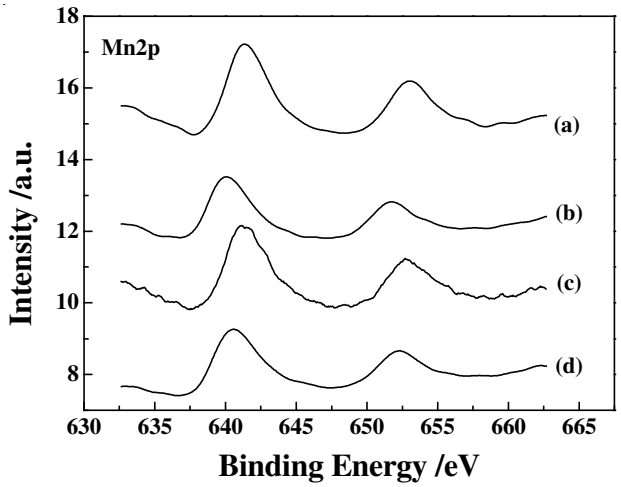

Fig. 3. XPS spectrum of Mn2p for $LaMn_{1-x}Cu_xO_3/Al_2O_3$: (a) x = 0.3, (b) x = 0.4, (c) x = 0.2, (d) x = 0

of copper and manganese ions in the perovskite-type structure of catalysts with XPS. The spectra for the Cu2p level of samples (not showing here) have the satellite peaks, which separate from the main peak by about 9 eV, so the valence state of copper ion at all catalysts was mainly considered as Cu^{2+}. The main peak positions of Cu2p of all the catalysts are the same binding energy. The spectra for the Mn2p level of the prepared catalysts investigated and showed in Fig. 3. The peak positions of the Mn2p level of catalyst with the x value of 0, 0.2, 0.3 and 0.4 are observed as 641.4, 640.9, 641.4 and 641.2 eV, respectively. Their multiple splitting of $Mn2p_{3/2}$ and $Mn2p_{1/2}$ are 11.6, 11.6, 11.7 and 11.7 eV, respectively. From these results, it seems to be difficult to discern the valence state of manganese ion in the catalyst, but the broaden of the $Mn2p_{3/2}$ peak and the shift of the peak position, which caused by the change of valence state from Mn^{3+}-Mn^{4+}, conforms to the mixed state of Mn^{3+} and Mn^{4+} in the substituted catalyst. La-Mn based samples prepared in air would form some Mn^{4+} ions in order to reduce the static Jahn-Teller distortion of Mn^{3+} and been accompanied by the formation of oxygen excess. This kind of over-stoichiometric oxygen (namely excess oxygen) associated with Mn^{4+} can be easily reduced due to its low coordination number with cation on perovskite lattice, resulting in the increase of catalytic activity. Some fraction of the Mn^{2+} was proposed to be exist in the catalyst with the x value of 0.4, the Mn^{2+} state results from the increase of lattice oxygen vacancies that caused by the partial substituted of Mn^{n+} with Cu^{2+} ion. It would be one reason for the higher catalytic activity of the $LaMn_{0.6}Cu_{0.4}O_3/Al_2O_3$ catalyst in catalytic combustion of ethyl acetate than other samples. The increase of the surface lattice oxygen vacancies weaken the interaction between adsorbed oxygen (O^-) and low coordinated metals (Mn and Cu) in the surface structure of $LaMn_{0.6}Cu_{0.4}O_3/Al_2O_3$, thus, the catalytic activity was highly enhanced.

In principle, besides surface atomic composition, XPS also provides information by position of the signals on the binding energy scale. In Table-3, there is no obvious difference between the binding energies of the elements and no apparition of new peaks observed. We can confirm that no specific chemical interaction of La^{3+} and Mn^{3+} of the active phase and Al_2O_3 support occurred. This is in good agreement with the data of XRD. The comparison between XPS and chemical La/Al ratios points to a preferential accumulation of deposited phase at the external surface of the support.

TABLE-3
VALUES OF BINDING ENERGY AND ATOM RATIO FROM XPS

Catalyst	X Value	La	Mn	Cu	Al2p	O1s	La/Al[a]	La/Al[b]
Cat. 0	0	834.73	641.35	–	73.28	530.36	0.70	0.05
Cat. 2	0.2	834.25	641.11	933.33	73.16	530.30	1.35	0.07
Cat. 3	0.3	834.19	641.35	933.27	73.10	530.24	1.29	0.06
Cat. 4	0.4	834.13	641.23	932.89	73.10	530.18	1.19	0.06

a: Ratio of La-Al from XPS, b: Chemical ratio of La-Al.

In Fig. 1, $LaMn_{0.6}Cu_{0.4}O_3/Al_2O_3$ catalyst shows the highest activity in the all samples. Therefore, the thermal stability of this sample investigated and the conversion of ethyl acetate as a function of reaction time shown in Fig. 4. Obviously, at low temperature range, the catalyst can sustain a long time with

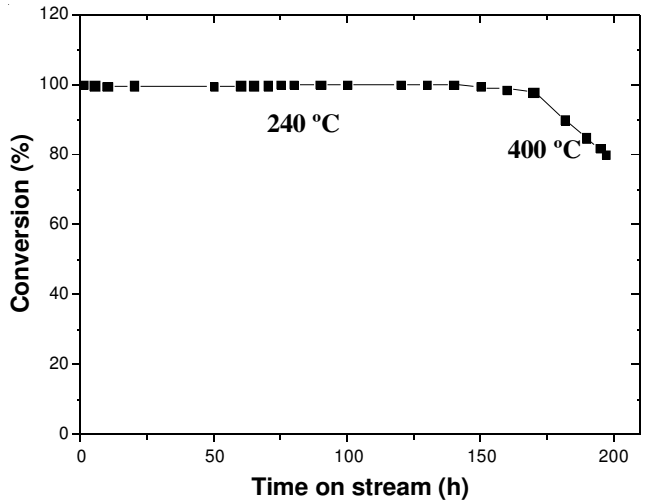

Fig. 4. Thermal stability for the catalysts

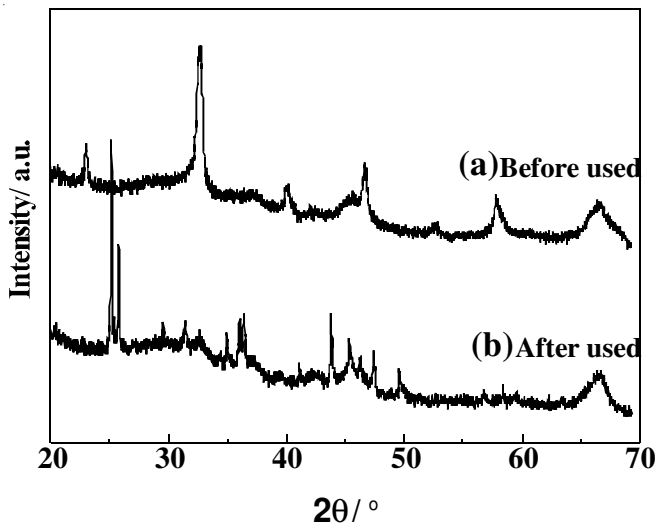

Fig. 5. XRD patterns of fresh and used catalyst

completely conversion. When the reaction temperature was increased to 400 ºC, the ethyl acetate conversion dramatically decreased after a few hours. The sharp decrease of the ethyl acetate conversion under this condition was mainly due to the catalyst structure transform. As Fig. 5 shows, after a long thermal stability test, the perovskite phase peak shifted obviously. We can suppose that the products, such as H_2O and CO_2 generated during the catalytic combustion, obviously affect the stability and the activity of the perovskite catalyst at comparatively high temperature. Thus, some further investigations should be done about this to improve the catalytic performance in the future.

Table-1 listed the results of combustion of ethyl acetate on $LaMn_{0.6}Cu_{0.4}O_3/Al_2O_3$ catalyst. The improving of the CO_2 selectivity with the increasing of $LaMn_{0.6}Cu_{0.4}O_3/Al_2O_3$ weight per cent not detected. The catalyst with 10 % loading showed the highest CO_2 selectivity than other samples. This may be due to the high dispersion of the perovskite phase covering on the support surface. We can see the aggregation of the perovskite with the loading of 20 % in Fig. 7. As for the sample with the loading of 5 %, catalytic combustion of ethyl acetate occurred on part of the exposed support surface, thus, some by-products were detected[10], such as ethanol and aldehyde. The low BET surface area resulted in the poor catalytic performance of the bulk perovskite catalyst. High dispersion of perovskite phase on the support is necessary to improve the selectivity and activity.

The XRD patterns of catalysts with different perovskite loadings shown in Fig. 6. The diffraction peaks of the Al_2O_3 are visible, but the formation of the perovskite structure only be detected on the sample with the loading of 20 % and the bulk sample. One reason is that the low amount of supported materials in the sample and the other being the presumable small size of crystallites or a poor crystalline, which confirmed by the SEM micrographs of Fig. 7. Combining with the results in Table-2, it is obviously that 10 % sample with smaller particles of the perovskite on the support surface shows higher selectivity and activity than that of the 20 % sample. In bulk perovskite prepared by the citrate process, a well-crystallized single phase could obtain at 580 ºC[23]. It is reported[24] that the perovskite-phase would well define and XRD detectable for lower loadings only after calcinations at 900 ºC. The mere fact is that the high temperature is necessary for sintering a poorly crystalline-deposited perovskite. We may thus confirm that the catalytic performances of perovskite-type catalyst greatly affected by such structure and the morphology.

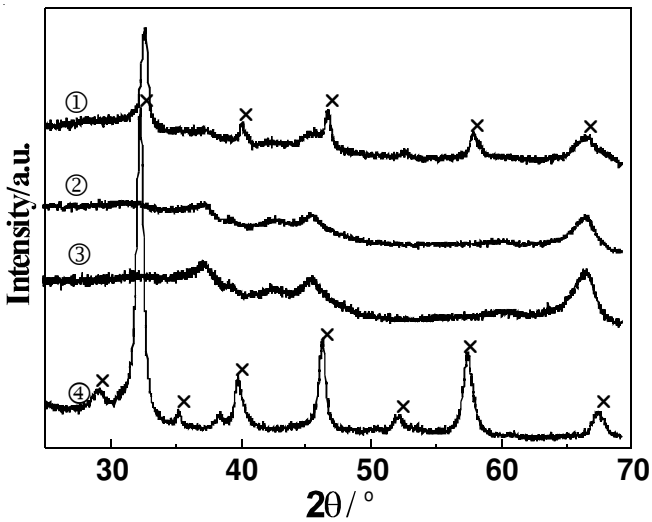

Fig. 6. XRD patterns of catalysts with the loading of ①20, ②10, ③5 and ④100 %

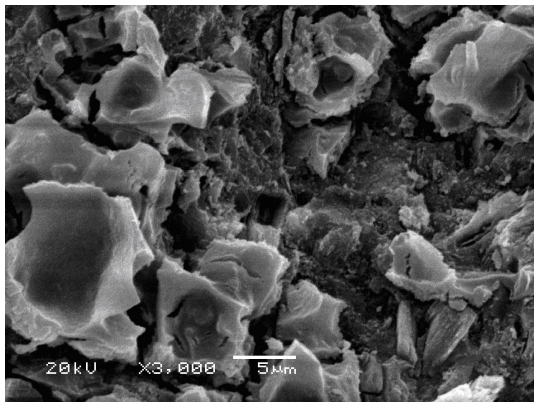

(a) 20 % $LaMn_{0.6}Cu_{0.4}O_3/Al_2O_3$

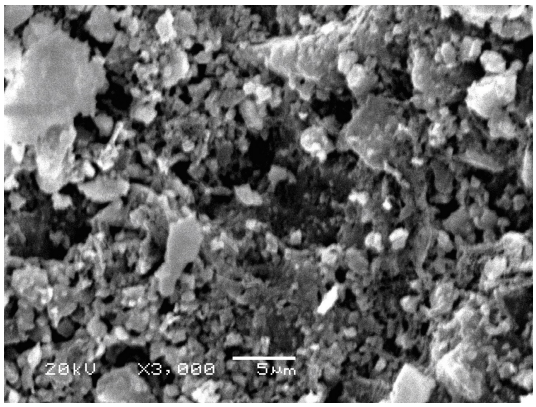

(b) 10 % $LaMn_{0.6}Cu_{0.4}O_3/Al_2O_3$

Fig. 7. SEM patterns of the catalysts with different perovskite loading

Conclusion

The results obtained in this work showed that Cu-substituted La-Mn based perovskite supported on γ-Al_2O_3 catalyst is an efficient catalyst for ethyl acetate complete catalytic oxidation. At 240 ºC, ethyl acetate completely converted exclusively into H_2O and CO_2 on the Cat. 4 ($LaMn_{0.6}Cu_{0.4}O_3/Al_2O_3$) sample and no catalyst deactivation observed after 150 h of test. The catalytic activity of the catalyst was highly enhanced with respect to the bulk perovskite sample. Detailed XRD and XPS analysis showed that the role of the Cu^{2+} substitution correlated with the formation of more Mn^{4+} cation and the fixation of the oxygen stoichiometry of the material. The different activities of the various catalysts were due to the changed contents and mobility of active oxygen of the catalyst, which induced by the partial substitution of Mn by Cu ion.

REFERENCES

1. P.Y. Lin, M. Skoglundh, L. Lowendahl, J.-E. Otterstedt, L. Dahl, K. Jansson and M. Nygren, *Appl. Catal. B*, **6**, 237 (1995).
2. L.G. Tejuca, J.L.G. Fierro and J.M.D. Tascon, *Adv. Catal.*, **36**, 237 (1989).
3. T. Seiyama, *Catal. Rev. Sci. Eng.*, **34**, 281 (1992).
4. L. Fabbrini, I. Rossetti and L. Forni, *Appl. Catal. B*, **56**, 221 (2006).
5. M. Alifanti, N. Blangenois, M. Florea and B. Delmon, *Appl. Catal. B*, **280**, 255 (2005).
6. M. Alifanti, M. Florea, S. Somacescu and V.I. Parvulescu, *Appl. Catal. B*, **60**, 33 (2005).
7. Y. Nan, C. Yong and S. Yang, *J. Catal.*, **230**, 249 (2005).
8. S. Cimino, R. Pirone and L. Lisi, *Appl. Catal. B*, **35**, 243 (2002).
9. M.A. Pena and J.L. Fierro, *Chem. Rev*., **101**, 1981 (2001).
10. D. Ferri and L. Forni, *Appl. Catal. B*, **16**, 119 (1998).
11. Y. NgLee, R.M. Lago, J.L.G. Fierro, F. Sapina and E. Martinez, *Appl. Catal. A*, **207**, 17 (2001).
12. Y. Ahang-Steenwinkel, J. Beckers and A. Bliek, *Appl. Catal. A*, **235**, 79 (2002).
13. M. Alifanti, R. Auer, J. Kirchnerova, F. Thyrion, P. Grange and B. Delmon, *Appl. Catal. B*, **41**, 71 (2003).
14. S. Royer, H. Alamdari, D. Duprez and S. Kaliaguine, *Appl. Catal. B*, **58**, 273 (2005).
15. H. Arai, T. Yamada, K. Eguchi and T. Seiyama, *Appl. Catal.*, **26**, 265 (1986).
16. D. Klvana, J. Kirchnerova, J. Chaouki, J. Delval and W. Yaici, *Catal. Today*, **47**, 115 (1999).
17. P.E. Marti and A. Baiker, *Catal. Lett*., **26**, 71 (1994).
18. R. Spinicci, A. Tofanari, M. Faticanti, I. Pettiti and P. Porta, *J. Mol. Catal. A*, **176**, 247 (2001).
19. K. Kniaek, M. Daturi, G. Busca and C. Michel, *J. Mater. Chem*., **8**, 1815 (1998).
20. P. Papaefthimiou, T. Ioannides and X.E. Verykios, *Catal. Today*, **54**, 81 (1999).
21. M.C. Álvarez-Galván, V.A. de la Peña O'Shea, G. Arzamendi, B. Pawelec, L.M. Gandía and J.L.G. Fierro, *Appl. Catal. B*, **92**, 445 (2009).
22. J.G. Deng, L. Zhang, H.X. Dai and C. Au, *Appl. Catal. A*, **352**, 43 (2009).
23. H.M. Zhang, Y. Teraoka and N. Yamazoe, *Chem. Lett*., 665 (1987).
24. H.M. Zhang, Y. Teraoka and N. Yamazoe, *Appl. Catal. B*, **41**, 137 (1988).